Magnetic resonance spectroscopy — Revisiting the biochemical and molecular milieu of brain tumors

Ashish Verma [a,*], Ishan Kumar [a], Nimisha Verma [b], Priyanka Aggarwal [c], Ritu Ojha [d]

[a] Department of Radiodiagnosis and Imaging, Institute of Medical Sciences, Banaras Hindu University, Varanasi 221005, India
[b] Department of Anesthesiology, Institute of Medical Sciences, Banaras Hindu University, Varanasi 221005, India
[c] Department of Pediatrics, Institute of Medical Sciences, Banaras Hindu University, Varanasi 221005, India
[d] Consultant Radiologist

ARTICLE INFO

ABSTRACT

Background: Magnetic resonance spectroscopy (MRS) is an established tool for in-vivo evaluation of the biochemical basis of human diseases. On one hand, such lucid depiction of 'live biochemistry' helps one to decipher the true nature of the pathology while on the other hand one can track the response to therapy at sub-cellular level. Brain tumors have been an area of continuous interrogation and instigation for mankind. Evaluation of these lesions by MRS plays a crucial role in the two aspects of disease management described above.
Scope of review: Presented is an overview of the window provided by MRS into the biochemical aspects of brain tumors. We systematically visit each metabolite deciphered by MRS and discuss the role of deconvoluting the biochemical aspects of pathologies (here in context of brain tumors) in the disease management cycle. We further try to unify a radiologist's perspective of disease with that of a biochemist to prove the point that preclinical work is the mother of the treatment we provide at bedside as clinicians. Furthermore, an integrated approach by various scientific experts help resolve a query encountered in everyday practice.
Major conclusions: MR spectroscopy is an integral tool for evaluation and systematic follow-up of brain tumors. A deeper understanding of this technology by a biochemist would help in a swift and more logical development of the technique while a close collaboration with radiologist would enable definitive application of the same.
General significance: The review aims at inciting closer ties between the two specialists enabling a deeper understanding of this valuable technology.

Contents

* Corresponding author.
  E-mail address: drdnv5@gmail.com (A. Verma).

1. Introduction

Alterations in biochemical pathways involved in causation and those resulting from occurrence of most human diseases have been understood to an extent and still remain an intriguing problem for clinical scientists. An assessment of the biochemistry of diseased human tissue can provide useful information to aid in diagnosis and grading/staging of diseases and, in monitoring of therapy. During the past two decades, various techniques have been employed for metabolic profiling of normal and pathological tissue such as gas chromatography–mass spectrometry (GC–MC), Fourier transform-infrared spectrometry (FT-IR), Liquid chromatography–mass spectrometry (LC–MS), Ramen spectroscopy, thin layer chromatography and nuclear magnetic resonance (NMR) spectroscopy [1]. Of these NMR mass spectrometry has the best sensitivity and can identify up to 160 metabolite peaks [2]. Proton MR Spectroscopy (H^{1}MRS) is an extrapolation of the above technology, focusing on the signals harnessed from spinning protons present in almost all molecules of human body. Best exploitation of the technique has been done in evaluation of brain diseases especially for neuro-oncology. The technique remains of vital importance for an initial in-vivo assessment of tumor characterization and grading, for follow-up on treatment of tumors where obtaining a biopsy sample for ex-vivo examination is not possible and in situations where complete resection of a tumor is not possible. Further H^{1}MRS finds increasing application in characterization of benign pathologies as well viz. tuberculoma, metabolic and demyelinating brain diseases. Presented is an overview of the basic principles, clinical extrapolations and applications of H^{1}MRS in the everyday clinical workflow, emanating from the unique window of non-invasive tissue interrogation provided by MRS. As per the common parlance most examples pertain to neuroradiological applications however that should not imply that equally.

2. Basic principles and technique of H^{1}MR spectroscopy

2.1. Basic principle

The identification of different chemicals in a tissue is based on the fact that protons in different molecules with different atomic numbers precess at different frequencies. This difference in frequencies (Larmor frequencies) is derived from the populace of electron cloud surrounding the protons. As electrons are charged particles, they show magnetic spin properties and when exposed to external magnetic field (B0) generates a small magnetic field (B*). As a result, magnetic environment surrounding the nucleus (and hence protons) is modified minimally (expressed in parts per million of the external magnetic field (B0). Consequently, the resonance frequency of the nucleus, which is directly proportional to the magnetic field it experiences, shifts. This phenomenon is known as chemical shift and forms the basis of MR spectroscopy [3].

2.2. Techniques

There are two basic techniques utilized in MR spectroscopy; single voxel techniques and multivoxel techniques. Single voxel techniques employs PRESS (point-resolved spectroscopy) or STEAM (stimulated-echo acquisition mode) sequences. STEAM offers advantages for the obtaining short TE resonant metabolites and more effective water suppression. The advantages of PRESS includes two-fold increase in obtained signal intensity, and lesser susceptibility to motion, homonuclear coupling effects, and eddy current [3,4]. Multivoxel imaging, also known as CSI (chemical shift imaging) and MRSI (MR spectroscopic imaging) can obtain spectra from a large volume of interest (VOI). CSI is better suited for evaluation of brain tumors because of their larger size and morphological and metabolic heterogeneity [5]. It also allows for comparison and normalization of pathologic spectra to spectra in normal tissue [6].

2.3. Choice of echo time (TE)

Short TE (20 to 40 ms) is useful in demonstrating myoinositol (MI), glutamine/glutamate (Glx), amino acids, lactate, and lipids. They are also useful in monitoring therapy for these diseases. Intermediate TE (135 to 144 ms) provides information on fewer metabolites, however, it has numerous advantages over short TE MRS such as differentiation of lactate/alanine peak from lipids at 1.3–1.5 ppm (inversion of lactate and alanine peaks occur at intermediate TE due to J coupling), better delineation of NAA peak at 2.0 to 2.05 range (superimposed Glx peak at 2 to 2.5 ppm on short TE), more accurate demonstration of lipid peak and choline peak and less base line distortion compared to short TE [3,6]. Long echo time (270 to 288 ms) produces less signal from NAA, Cho and creatinine and can be used to depict lactate peaks accurately; however, has lesser signal to noise ratio [7]. The current recommendation is to acquire short TE and of time permits, intermediate TE acquisitions. [6].

3. Which neurochemicals can be identified in H^1 MRS spectrum of normal brain and brain tumors

Every molecule exhibits its own fingerprint on the chemical shift spectrum. Understanding and identifying these frequency profiles forms the first step in evaluation of MR spectroscopic data.

3.1. Lipids

Beginning from the lower frequencies the first resonant peak of clinical interest are of lipids which resonate at 0.9 ppm (CH3) and 1.3 ppm ((CH2)n). These lipids are known as NMR visible mobile lipids (ML). The rise of lipids detected in various cellular processes such as necrosis, growth arrest, inflammation, malignancy and apoptosis. Membrane lipids are usually not recognized on standard MRS unless

imaged at very short echo time [3,8]. The lipid peaks detected in most of these processes are predominantly saturated lipids believed to arise from increased number of cytoplasmic vesicles especially in tissues demonstrating necrosis and inflammation. The presence of lipid in lymphoma is postulated to arise from increased membranous component in transformed lymphoid cells [9]. The presence of lipids in the spectra also correlates well with the increased proportion of cells in S and G2 phase of cell cycle signifying growth arrest [10,11]. Various in-vivo and in-vitro MRS studies have showed that lipid peak obtained during apoptosis is predominantly polyunsaturated fatty acids which are primarily constituents of mitochondrial membrane [12]. Lipid peaks have been demonstrated in craniopharyngioma corresponding to high amounts of cholesterol in the cyst fluid [13].

3.2. Lactate

CH3 (methyl group) of lactate produces doublet peak at 1.33 ppm which points upward at short TE and downwards at intermediate TE. Lactate is an end product of glycolysis and increases rapidly during hypoxia and ischaemia, in particular as a result of poor vascularity and acquired resistance to hypoxia. Increased rates of lactate production are associated with a range of tumors and usually signifies higher tumor grade and correlates with tumor metabolic activity. Lactate peak usually is absent in low grade brain tumors and is constituent of classical MR spectroscopy signature for a high grade primary brain tumor [14].

3.3. Alanine

Alanine results into a doublet peak at 1.47 ppm which inverts at intermediate TE due to J coupling. Another small singlet peak of alanine is found at 3.93 ppm. Alanine peak is produced by transamination of pyruvate in hypoxic tissues showing increased glycolysis to prevent further increase in lactate [15]. Amongst the brain tumors, meningiomas show a distinct alanine peak with variable sensitivity. Alanine in meningiomas has been postulated to be a partial oxidation of glutamine [16]. or converted from increased pool of pyruvate due to inhibitions of the enzyme pyruvate kinase by L-alanine [17]. Alanine peak is also elevated in central neurocytoma and PNET [18–20].

3.4. Acetate and succinate

Acetate demonstrates a singlet peak at 1.92 ppm while succinate shows a singlet peak at 2.42 ppm. Raised acetate and succinate levels reflect anaerobic fermentation of pyruvate generated from glycolysis where it undergoes carboxylation to form acetate and succinate. Although these peaks might be slightly raised in brain tumors, clinically the presence of markedly raised acetate and succinate peaks in the MR spectra is useful for identifying brain abscesses that mimic brain tumors on conventional MR. [21,22].

3.5. N-acetyl aspartate (NAA)

N-acetyl aspartate (NAA) shows the largest peak of the spectra at 2.02 ppm as a singlet peak and another quadruplet peak at 2.5 ppm. NAA peak also obtains contributions from N-acetyl aspartyl glutamate (NAAG), glycoproteins, and amino acid residues in peptides. NAA is the second most abundant amino acid in the brain and is synthesized in mitochondria from aspartate and acetyl CoA and is transported into the cytosol, where it is converted into aspartate and acetate by the enzyme aspartoacylase [3,23–26]. Although exact role of NAA in human brain metabolism is uncertain, on the animal model studies it is postulated to be involved in lipogenesis pathways, coenzyme A (CoA) interactions [27–28]. Immunocytochemistry confirms that NAA is located primarily in neuronal tissues, hence can be used a surrogate marker for neuronal density and integrity. In all the pathologies causing axonal loss including malignant or benign tumors, NAA is markedly reduced or even absent. Lack of the biosynthetic enzyme for NAA, Asp-NAT (aspartate N acetyltransferase) within the brain tumors is deemed as an explanation for the lack of NAA signals [29]. Central neurocytoma, an uncommon neuronal tumor, have been reported to exhibit detectable NAA peak, although with decreased NAA/Cr [20,30]. NAA peaks have also been used in predicting the histological type of the hypothalamic hamartomas with higher NAA in the hamartomas with mainly neuronal content compared to those with glial content [31].

3.6. GLX

GLX consists of glutamate (glu), glutamine (gln) and GABA peaks. Beta CH2 and Gamma CH2 moieties produce 2.0–2.46 ppm and alpha CH group at 3.6–3.8 ppm. Glx complex has been observed in peritumoral brain edema which is consistent with underlying demyelination and neuronal loss [32]. GLX can aid in differentiation of oligodendroglioma from astrocytomas as it is reported to be significantly higher in oligodendrogliomas [33].

3.7. Creatine

Creatine peak is seen at 3.03 ppm with primary contributions from creatine and phosphocreatine and minor contributions from GABA, lysine, and glutathione [34,35]. Another creatine peak is observed at 3.93 ppm. Cr signal is a marker for intracellular energy states as it stores high energy phosphates. In the clinical MR spectroscopy Cr peak is utilized as internal reference standard for characterizing other peaks as its level is high and relatively comparable in different tissue types of brain [36]. However, literature suggests that glial tumors show 15–40% reduction in Cr levels. Similar data has been reported in various other tumors as well, such as meningotheliomatous meningiomas which shows approximately 20% reduction in total creatine [37,38]. Total creatine content is significantly low in non-neuroectodermal tumors such as brain metastases compared to neuroectodermal tumors [37].

3.8. Choline containing metabolites (CCM)

The Choline (cho) resonance is present approximately at 3.2 ppm and 3.52 ppm. The resonance is attributed to trimethyl ammonium residues of free choline (3.21 ppm), phosphorylcholine (3.23 ppm), glycerophosphorylcholine (3.24 ppm) and other metabolites such as carnitine [39]. These frequency assignments of individual Cho constituents have been tentatively assigned by various researchers; however, it is yet unresolved by scanners approved for clinical use. Cho is a salient component of the Kennedy pathway, involved in genesis of phospholipid of the cell membranes. Cho is phosphorylated by Choline Kinase (CK) to from PCho which reacts further with CTP to yield CDP-choline. Phosphatidylcholine (PC) then results from the reaction of CDP-choline with diacylglycerol [40]. The enzyme Choline Kinase is overexpressed in several brain tumors and hence the presence of choline peak in MRS spectra reflects increased cell membrane synthesis and thus increased cellularity [41,42]. Miller and colleagues report that the CCM peak obtained in brain tumor specimen correlates with Cho, PCho, GPCho but not phosphatidyl choline [41].

Different authors have suggested different approaches to quantitative assessment of choline peak. Some recommend Cho/cr ratio comparison with the contralateral normal parenchyma [43] whereas others have reported better correlation of Cho/NAA with the tumor grade [44,45]. Some studies have emphasized that even NAA and Cr levels decrease during tumor progression producing erroneous underestimation of tumor progression using these ratios [46].

3.9. Taurine

Taurine shows two triplet peaks at 3.25 and 3.43 ppm. It is an inhibitory neurotransmitter that activates GABA-A receptors or strychnine-sensitive glycine receptors [47]. Increased taurine is seen in PNET, medulloblastoma, pituitary microadenoma and metastatic renal cell carcinoma. High levels in medulloblastoma points towards morphogenetic similarities between medulloblastoma and retinoblastomas as retina contains one of the highest levels of taurine owing to the presence of its high affinity transport system [48,49].

3.10. Myoinositol

Myoinositol produces at a quadruplet peak at 3.55 ppm. This is believed to be an osmolyte that is found primarily in astrocytes. In tumors, myoinositol is involved in osmoregulation and volume regulation. Increased levels of mI are believed to reflect increased numbers of glial cells, which have been reported to contain high levels of mI, and in particular have been reported to be high in grade II gliomas [5]. Castillo and colleagues have observed that myoinositol is relatively higher in low-grade gliomas (grade II gliomas) and lower in higher grade tumors such as anaplastic astrocytoma (grade III) and glioblastoma multiforme (grade IV gliomas) [50]. Krieger and colleagues have reported that MI detected within an intraventricular tumor in a pediatric patient suggests choroid plexus papilloma [51].

3.11. Glycine

Glycine is an amino acid which resonates at 3.55 ppm. High levels of glycine are found in medulloblastoma, ependymoma, glioblastomas and central neurocytoma [52]. Studies show that high glycine synthesis in gliomas is due to highly activated serine hydroxymethyltransferase (SHMT) or deficiency of hypoxanthine–guanine phosphoribosyltransferase within the glioma cells [53–55]. Regardless of necrotic component glycine peak is significantly high in glioblastoma, differentiating them from metastatic lesions [37].

3.12. Glucose

(C2–C6 protons) resonate in 3.43–3.8 ppm range but the signals are usually low and undetectable at 1.5 T magnets except for some low grade glioma [56].

4. The spectra of different brain tumors

4.1. Intraparenchymal tumors: biochemical milieu of glial tumors (Fig. 1)

MR spectra of glial tumors show decreased total creatine, nearly absent to markedly reduced NAA, raised choline and choline containing compounds and a prominent glycine peak [37]. Ex-vivo studies have shown raised levels of PEA in the glioma cells which can be attributed to breakdown of phosphatidyl-ethanolamine in order to produce DAG (diacyl glycerol) which acts as a second messenger system to invoke cellular proliferation via phospholipase c [57]. Differentiation of glial tumors from cerebral metastasis can be obtained with the hypothesis that the peritumoral edema surrounding the brain metastasis is purely vasogenic whereas the edema surrounding high grade gliomas shows tumoral infiltration. Elevated choline and reduced creatinine can be found in peritumoral edema in gliomas compared to metastases [58]. MRS may also aid in identification of cerebral metastatic origin. An interesting study [59] has reported that secondaries from colorectal carcinoma metastases show a higher lipid content and suggest a threshold value of 2 for lipid/creatine ratio for its identification.

A lipid dominated spectrum in the absence of tumoral necrosis is found in lymphomas which are suggested to be due to macrophase accumulation along with increased membranous component in transformed lymphoid cells containing high levels of mobile lipids [9]. Another consistent finding demonstrated by brain lymphomas is the increase in choline resonance within the tumor and peritumoral areas
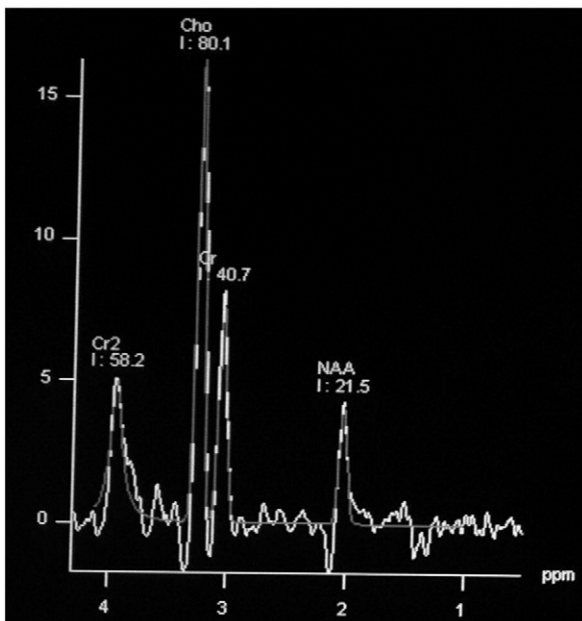

Fig. 1. H[1]MRS spectra acquired at intermediate TE (135ms) shows elevated choline at 3.2 and a decreased NAA peak at 2.02, presence of an inverted lactate peak at 1.3 indicates anaerobic metabolism. Note the presence of elevated myo-inositol (mI) at 3.56. Such a spectra correlates well with the possibility mentioned above as less aggressive metabolism on MRS corresponds to a moderate to low grade (WHO) tumor with elevation of mI correlating to possibility of an oligodendroglial tumor.
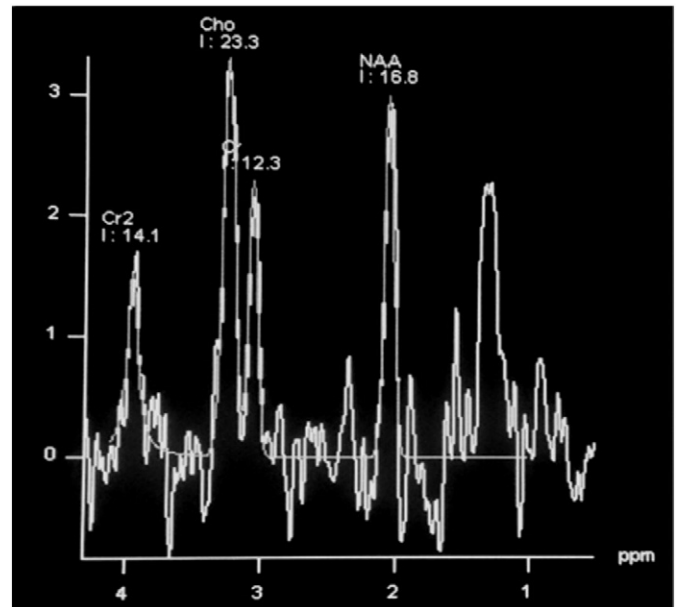

Fig. 2. H[1]MRS spectra acquired at intermediate TE (135ms) in a pediatric brain stem tumor diagnosed as glioma. A non-specific spectra with an elevated choline at 3.2 and a decreased NAA peak at 2.02 with presence of a lipid peak at 1.3. Though these features are non-specific however presence of lipid with elevation of choline indicates an aggressive nature of tumor (which may point towards grade shift). The diagnosis of pediatric brain stem glioma remains obvious on imaging, the need of MRS if at all is for grading of tumor.

[16]. Chawla et al. have suggested a higher lipid + lactate/creatine ratio with threshold >7.09 observed in peritumoral regions of lymphomas compared to glial tumors [69]. Lymphomas (Fig. 4) contain high PEA content due to their high content in lymphatic tissues. Studies have shown that PEA (phosphoryl ethanolamine) can be measured in-vivo using 1H-decoupling technique [70].

4.2. Assessment of tumor grade (Fig. 2)

There are various studies that correlate choline levels with the grade of glial tumors. Anaplastic astrocytomas (WHO grade III) are found to have higher choline levels compared to low grade gliomas [60]. A ratio of NAA/tCHO has been suggested as an accurate index to discriminate between low grade and high grade (grade III) astrocytomas with ratio > 1.6 predicting high grade gliomas [61,62]. Nevertheless there are tangible discrepancies between the various studies correlating choline levels and grade of gliomas. Lactate and lipids have been found in high grade necrotic tumors but with variable consistency [60,63,64]. mI and glycine have been reported to play significant role in grading of the glial tumors. mI and glycine both appear at 3.5 ppm at short TE, however mIdisappears at intermediate TE whereas glycine persists. The level of glycine increases with the grade of glial tumor [63,65] whereas the level of mI is high in low grade gliomas [60]. Candiota et al. have developed an (mI + Gly) / CR index to grade glial tumors while voxel is being placed on cellular part of the mass with the ratio decreasing significantly between low grade glioma and high grade glioblastoma [66].

4.3. Biochemical follow-up: relevance of MRS (Fig. 3)

MRS detected metabolite alteration can differentiate between disease progression and pseudo-progression/radiation necrosis, the latter often resembling the former on conventional MR sequences. More aggressive and revised treatment strategy has to be followed in tumor progression while pseudo-progression/radiation necrosis mandates observation on maintenance of the therapy [63]. About 1.7 to 1.8 times elevation of choline over either NAA or creatine may be utilized to predict tumor progression with high accuracy [67,68]. This may be complimented further by newer functional MR techniques like diffusion and perfusion weighted imaging.
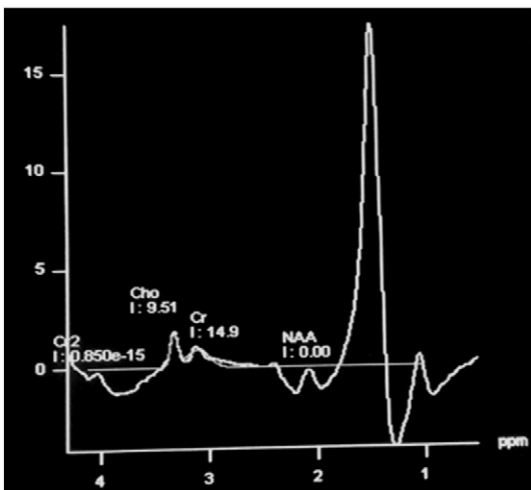

Fig. 4. H[1]MRS spectra acquired at intermediate TE (135ms) shows a spectra with an elevated choline at 3.2 and a decreased NAA peak at 2.02. A prominent lipid peak at 1.3 in the presence of choline in a tumor indicates a possibility of lymphoma.

4.4. Spectroscopy in extraparenchymal mass (Figs. 5,6)

Most extraparenchymal tumors are benign meningioma which can be easily identified on conventional MR sequences and CT scan with a reasonable certainty. Urgent surgical intervention is not necessary and patients can even be subjected to follow up. However before acquiring such an approach, one must be mindful of the conditions that may mimic these lesions that may not be benign. On MRS meningioma
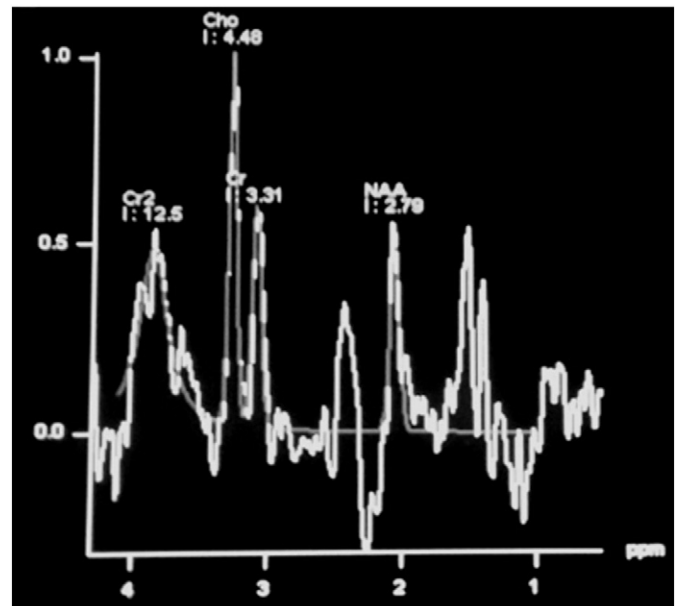
Fig. 5. H[1]MRS spectra acquired at low TE (30ms) shows an elevated alanine peak at 1.48 ppm proposing a possibility of meningioma. This is the first peak seen in the spectra (after lipid at 1.3) following which the NAA peak is reduced as meningioma is an extra-axial tumor (the NAA seen is due to contamination from adjacent brain). Note the prominent choline peak with a small creatine peak, which signifies a hyppometabolic tumor.

Fig. 3. H[1]MRS spectra acquired at intermediate TE (135ms) in a follow up case of glioblastoma multiformis showing a prominent lipid peak at 1.3 ppm. No other significant peak is seen. Such a spectra in a post-therapy scenario remains quite specific and help in differentiating an area of radiation necrosis from tumor recurrence.
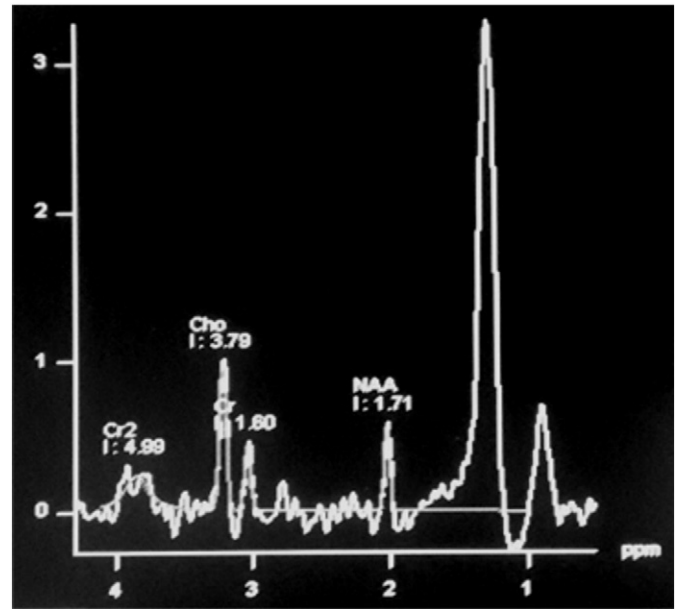
Fig. 6. H[1]MRS spectra acquired at intermediate TE (135ms) in a suspected metastasis (a case of lung cancer) shows a non-specific spectra with an elevated choline at 3.2 and a decreased NAA peak at 2.02, presence of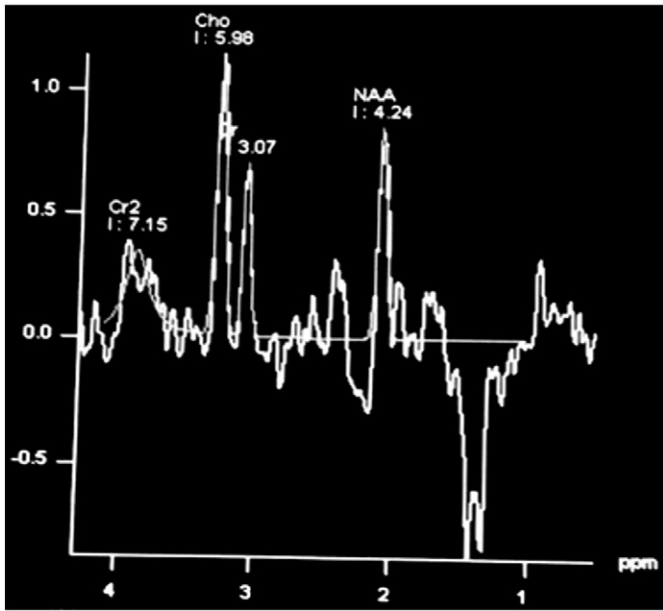 an inverted lactate peak at 1.3 indicating anaerobic metabolism. Significant choline elevation indicates a high cell membrane turn over while reduced NAA in an intra-axial tumor raises a suspicion of non-neurological origin of the lesion. A situation where an intra-axial lesion also behaves like being 'extra-axial', as the NAA seen is due to voxel contamination from adjacent brain rather than intra-tumoral signal, this can be noted while evaluating the voxel. This correlates with a possibility of secondary deposit, especially so if a primary is known.

shows prominent choline, nearly absent NAA or Creatine, and presence of alanine [71]. Alanine is considered a specific for meningioma but its identification rate is variable from 32 to 100% [16]. A distinct peak at 3.8 ppm has been suggested to reliably distinguish meningioma from other malignant tumors such as metastases or glioma. This peak has been suggested to correspond from Glx peak or from phosphoethanolamine and amino acids by ex vivo studies [72].

A proportion of meningeal tumors such as atypical meningiomas, atypical meningiomas, metastasis, and hemangiopericytomas are aggressive in nature and need early treatment or resection [63]. Hemangiopericytomas show high peak at 3.56 ppm at short TE which reduces in amplitude on long TE, corresponding to the myoinositol whereas meningiomas do not show this peak [73]. Malignant meningiomas (atypical and anaplastic meningiomas) are reported to show increased lipid peaks at short and long TE unlike the benign meningiomas [74,75]. Neurocytoma on the contrary is characterized by a glycine peak at 3.55 with moderate elevation of choline and reduction of NAA & creatine [52].

5. Limitations of MRS

MR spectroscopy is a technique with elegant physical principles and clinical extrapolations yet it suffers with certain inherent limitations. Physiological and non-physiological motion in human body causes an increased line widths, overall frequency shifts, reduced peak areas, and decreased quality of water suppression. These in turn lead to signal degradation and diminution and a resulting noisy spectra which remains inappropriate for clinical interpretation. Parallel imaging techniques with motion correction/compensation would go a long way to overcome the problem. Secondly, field in-homogeneities due to intrinsic (patient related) and extrinsic (hardware related) factors are reflected in the spectra as overlapping peaks. This causes poor peak
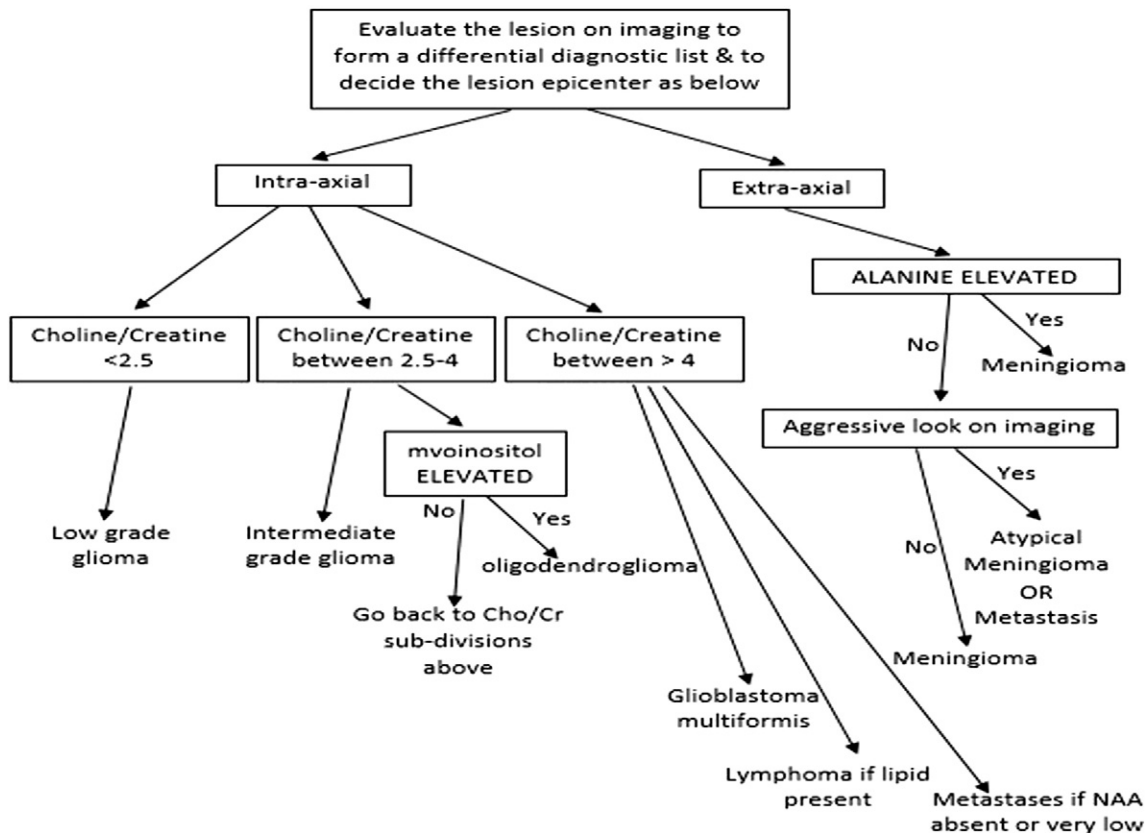

Fig. 7. MRS based proposed diagnostic algorithm for lesion differential diagnosis. The same should however be done primarily on the imaging features, contribution from functional imaging modalities like MRS should only to sought for correlation and problem solving purposes.

identification and quantification. The issue can be addressed by better active and passive shimming and by improving the overall field strength of the basic magnet. Truncation artifacts or sinc wiggles remain a major problem both in routine sequences as well as MRS. This causes baseline undulations to increase to an extent of masking the peak. Better receiver systems in RF antennae however can improve upon this limitation. Lastly, micro-metabolites and metabolites with very short signal decay time are difficult to pick up on clinically available scanners and mandate very high field strength magnets and gradient systems for detection [14,15,16,56,62].

6. Future directions

6.1. Multinuclear MRS

Several other nuclei have been applied and studied for MRS including helium-3 (3HE), lithium-7 (7Li), carbon-13 (13C), oxygen-17 (17O), fluorine-19 (19F), sodium-23 (23Na), phosphorus-31 (31P), and xenon- 129 (129Xe). Of these nuclei 31P 19F, and 13C have exhibited promise in the field of neuro-oncologic applications [6,76]. 31P MRS demonstrates seven major metabolite signals that are markers of energy consumption and transmittal within the brain cells and can be used as surrogate markers of intracranial energy reserves. These metabolites include three peaks of ATP, seen at -7.8, -16.3 and -2.7 ppm, Phosphocreatine (PCr) at 0 ppm, Phosphodiester (PDE) at 2.6 ppm, inorganic phosphate (Pi) at 4.9 ppm and Phosphomonoester (PME) at 6.5 ppm [77,78]. While ATP, PCr and Pi compounds reflect cellular energy metabolism, PDE and PME constitute membrane phospholipids. 31 P MRS also proves information about tissue pH by assessing the chemical shift of the inorganic phosphate signal relative to the Phosphocreatine signal. High grade gliomas show increased pH (alkalization), increase in PME, decrease in PDE/α-ATP and relatively unperturbed PCr/α-ATP or PCr/Pi ratios [3,6,79–81]. Meningiomas are characterized by an alkalinity (pH 7.16), a decrease in phosphocreatine, and decreased phosphodiesters [6]. However results are highly variable and some researchers have debated the role of tissue pH in tissue characterization as inconsistent and non-conclusive [82]. Recent studies have shown that NMR spectroscopy can be used to monitor the functions of gene products in various tumors. In a study on mice hepatoma cells comparing HIF-1 deficient tumor cells and those with wild type cells showing similar T2 relaxation measurements, in-vivo and ex-vivo NMR spectroscopy showed that HIF-1 deficient cells showed fivefold increase in total ATP and triple times increased PDE/Pi ratio indicating that HIF-1 primarily increases rate of glucose metabolism rather than promoting angiogenesis, as was previously thought [1,83].

Ultra-high-field MRS (beyond 3 T): obtaining neurospectrometric data at ultra high field (4 T and 7 T) scanners offers two-fold advantage of gain in signal to noise ratio (SNR) and increased chemical shift dispersion leading to consequent unambiguous identification of the metabolites [84]. Although the safety and clinical applications is still under investigation, early research is promising and likely to have a place in the future [6,85].

With the advent of high field strength magnets and faster RF detection systems, direct fourier transformation of free induction decay generated (FID) signal is another technique [82,83]. Signal from FID of H^1 resonance, generated in solid state NMR, decays over microseconds hence detection of the same to generate spectroscopic graph should be fast and sensitive. FID generated MRS remains a useful technique to assess lesions with homogenous physio-chemical properties as the limited number of frequencies decaying can be analyzed directly and quantified accurately [82–85]. Further, improved spectral resolution offered by advanced MR hardware can lead to detection of 'oncometabolites' like D-2-hydroxy glutarate (2-HG) which accumulates in IDH mutated gliomas due to 'gain-in-function' mutation in the gene coding for the enzyme isocitrate dehydrogenase (IDH). Once generated such metabolites compete with other energy metabolism enzymes and cause post-translational modification of proteins thereby rendering the tumoral milieu less sensitive to conventional therapy. Detection of oncometabolites can help plan and prognosticate the therapy in an evidence based manner. [86].

Functional MR spectroscopy is the new exciting advancement which facilitates surveillance of temporal changes in metabolite concentrations during various activities [3]. A technique named as PEPSI (proton echo planar spectroscopic imaging) has been described by Richards et al. for ultrafast repetitive spectroscopic assessment over a time period [87].

7. Conclusion

MR spectroscopy has transitioned from its infancy and is no longer a technological curiosity. With the advent of currently used high field scanners it has gained an unrivaled position in non-invasive assessment of biochemistry of the brain tumors as well as in fundamental and clinical research. Obviating the need for invasive chirurgical tissue sampling, MRS continues to provide substantial and useful insight into metabolomics of the brain tumors. We present a diagnostic algorithm which may assist in sub-classification of lesions once a list of differential diagnosis has been tailored as per the imaging appearance (Fig. 7). It is noteworthy that imaging appearance remains the primary tool to lateralize, localize and characterize the lesion with MRS playing a significant role in sub-classification of the biochemical mileu of upfront and treated brain tumors.

Transparency document

The Transparency document associated with this article can be found, in online version.

References

[1] J.L. Griffin, J.P. Shockcor, Metabolic profiles of cancer cells, Nat. Rev. Cancer 4 (2004) 551–561.
[2] E. Jellum, I. Bjornson, R. Nesbakken, E. Johansson, S. Wold, Classification of human cancer cells by means of capillary gas chromatography and pattern recognition analysis, J. Chromatogr. 217 (1981) 231–237.
[3] J. Pillai, L. Kwock, A. Horsk, Brain Magnetic Resonance Spectroscopy, in: J.R. Haaga, C.F. Lanzieri, R.C. Gilkeson (Eds.),CT and MR Imaging of the Whole Body, Vol. 1 2003, pp. 371–395.
[4] C.T.W. Moonen, P.C.M. van Zijl, J.A. Frank, et al., Comparisons of single shot localization methods (STEAM and PRESS) for in vivo proton NMR spectroscopy, NMR Biomed. 2 (1989) 201–208.
[5] A. Horská, P.B. Barker, Imaging of brain tumors: MR spectroscopy and metabolic imaging, Neuroimaging Clin. N. Am. 20 (3) (2010) 293–310.
[6] American College of Radiology, American Society of Neuroradiology, Society of Pediatric Radiology: ACR-ASNR-SPR practice guideline for the performance and interpretation of magnetic resonance spectroscopy of the central nervous system, revised, 2013 Retrieved from http://www.acr.org/~/media/ACR/Documents/PGTS/guidelines/MR_Spectroscopy.pdf.
[7] T. Lange, U. Dydak, T.P. Roberts, H.A. Rowley, M. Bjeljac, P. Boesiger, Pitfalls in lactate measurements at 3 T, AJNR 27 (2006) 895–901.
[8] M. Castillo, L. Kwock, J. Scatliff, S.K. Mukherji, Proton MR spectroscopy in neoplastic and non-neoplastic brain disorders, Magn. Reson. Imaging Clin. N. Am. 6 (1998) 1–20.
[9] Y.Z. Tang, T.C. Booth, P. Bhogal, et al., Imaging of primary central nervous system lymphoma, Clin. Radiol. 66 (8) (2011) 768–777.
[10] L.G. Astrakas, D. Zurakowski, A.A. Tzika, M.K. Zarifi, D.C. Anthony, U. De Girolami, et al., Noninvasive magnetic resonance spectroscopic imaging biomarkers to predict the clinical grade of pediatric brain tumors, Clin. Cancer Res. 10 (2004) 8220–8228.
[11] M.F. Veale, N.J. Roberts, G.F. King, N.J. King, The generation of 1H NMR-detectable mobile lipid in stimulated lymphocytes: relationship to cellular activation, the cell cycle, and phosphatidylcholinespecific phospholipase C, Biochem. Biophys. Res. Commun. 239 (1997) 868–874.
[12] J.L. Griffin, et al., Assignment of 1H nuclear magnetic resonance visible polyunsaturated fatty acids in BT4C gliomas undergoing ganciclovir-thymidine kinase gene therapy-induced programmed cell death, Cancer Res. 63 (2003) 3195–3201.
[13] R.N. Sener, M.R. Proton, Spectroscopy of Craniopharyngiomas, Comput. Med. Imaging Graph. 25 (2001) 417–422.
[14] M.E. Mullins, MR spectroscopy: truly molecular imaging; past,present and future, Neuroimaging Clin. N. Am. 16 (4) (2006) 605–618.
[15] O. Ben-Yoseph, R.S. Badar-Goffer, P.G. Morris, H.S. Bachelard, Glycerol 3-phosphate and lactate as indicators of the cerebral cytoplasmic redox state in severe and

mild hypoxia respectively: a 13C- and 31P-n. M. R. Study, Biochem. J. 291 (1993) 915–919.

[16] E. Kousi, I. Tsougos, E. Kapsalaki, Proton Magnetic Resonance Spectroscopy of the Central Nervous System, Novel Frontiers of Advanced Neuroimaging, InTech 2013, pp. 19–50.

[17] M. Castillo, J.K. Smith, L. Kwock, Correlation of myo-inositol levels and grading of cerebral astrocytomas, AJNR Am. J. Neuroradiol. 21 (9) (2000) 1645–1649.

[18] T. Krishnamoorthy, V.V. Radhakrishnan, B. Thomas, et al., Alanine peak in central neurocytomas on proton MR spectroscopy, Neuroradiology 49 (7) (2007) 551–554.

[19] C. Majos, J. Alonso, C. Aguilera, et al., Proton magnetic resonance spectroscopy ((1)H MRS) of human brain tumours: assessment of differences between tumour types and its applicability in brain tumour categorization, Eur. Radiol. 13 (3) (2003) 582–591.

[20] M.T. Chuang, W.C. Lin, H.Y. Tsai, et al., 3-T proton magnetic resonance spectroscopy of central neurocytoma: 3 case reports and review of the literature, J. Comput. Assist. Tomogr. 29 (5) (2005) 683–688.

[21] M. Garg, R.K. Gupta, M. Husain, et al., Brain abscesses: etiologic categorization with in vivo proton MR spectroscopy, Radiology 230 (2004) 519–527.

[22] P.H. Lai, K.T. Li, S.S. Hsu, et al., Pyogenic brain abscess: findings from in vivo 1.5-T and 11.7-T in vitro proton MR spectroscopy, Am. J. Neuroradiol. 26 (2005) 279–288.

[23] A.J. Barkovich, Pediatric Neuroimaging, second ed. Lippincott-Raven, Philadelphia, 1996 47–52.

[24] M. Benuck, J.A.F. D'Adamo, Acetyl transport mechanisms: metabolism on N-acetyl-l-aspartic acid in the non-nervous tissues of the rat, Biochim. Biophys. Acta 152 (1968) 611–618.

[25] K.M. Cecil, Technical Aspects of Performing and Interpreting Proton MR Spectroscopy (Syllabus, Advanced Imaging Symposium: Preparing the Neuroradiologist for the New Millennium, Pp 29–36), Paper Presented at Annual Meeting of the American Society of Neuroradiology, Atlanta, 2000.

[26] C.A. Davie, C.P. Hawkins, G.J. Barker, et al., Serial proton magnetic resonance spectroscopy in acute multiple sclerosis lesions: part 1, Brain 117 (1994) 49–58.

[27] S.J. Austin, A. Connelly, D.G. Gadian, et al., Localized 1H NMR spectroscopy on Canavan's disease: a report of two cases, Magn. Reson. Med. 19 (1991) 439–445.

[28] R. Burri, C. Steffen, N. Herschkowitz, N-acetyl-l-aspartate is a major source of acetyl groups for lipid synthesis during rat brain development, Dev. Neurosci. 13 (1991) 403–411.

[29] J.R. Moffett, B. Ross, P. Arun, C.N. Madhavarao, A.M.A. Namboodiri, N-Acetylaspartate in the CNS: from neurodiagnostics to neurobiology, Prog. Neurobiol. 81 (2) (2007) 89–131.

[30] R. Jayasundar, T. Shah, S. Vaishya, V.P. Singh, C. Sarkar, In vivo and in vitro MR spectroscopic profile of central neurocytomas, J. Magn. Reson. Imaging 17 (2003) 256–260.

[31] D.R. Amstutz, S.W. Coons, J.F. Kerrigan, H.L. Rekate, J.E. Heiserman, Hypothalamic hamartomas: correlation of MR imaging and spectroscopic findings with tumor glial content, AJNR Am. J. Neuroradiol. 27 (2006) 794–798.

[32] R. Ricci, A. Bacci, V. Tugnoli, et al., Metabolic findings on 3 T 1H-MR spectroscopy in peritumoral brain edema, AJNR Am. J. Neuroradiol. 28 (7) (2007) 1287–1291.

[33] M. Rijpkema, J. Schuuring, et al., Characterization of oligodendrogliomas using short echo time 1H MR spectroscopic imaging, NMR Biomed. 16 (1) (2003) 12–18.

[34] R. Kreis, B.D. Ross, Cerebral metabolic disturbances in patients with subacute and chronic diabetes mellitus: detection with proton MR spectroscopy, Radiology 184 (1992) 123–130.

[35] R. Kreis, B.D. Ross, N.A. Farrow, Z. Ackerman, Metabolic disorders of the brain in chronic hepatic encephalopathy detected with H-1 MR spectroscopy, Radiology 182 (1992) 19–27.

[36] D. Lu, S.G. Pavlakis, Y. Frank, et al., Proton MR spectroscopy of the basal ganglia in healthy children and children with AIDS, Radiology 199 (1996) 423–428.

[37] Y. Kinoshita, A. Yokota, Absolute concentrations of metabolites in human brain tumors using in vitro proton magnetic resonance spectroscopy, NMR Biomed. 10 (1) (1997) 2–12.

[38] O.H. Lowry, S.J. Berger, M.M.Y. Chi, A. Blackshaw, W. Outlaw, Diversity of metabolic patterns in human brain tumors. I. High energy phosphate compounds and basic composition, J. Neurochem. 29 (1977) 959–977.

[39] J. Urenjak, S.R. Williams, D.G. Gadian, Noble M proton nuclear magnetic resonance spectroscopy unambiguously identifies different neural cell types, J. Neurosci. 13 (3) (1993) 981–989.

[40] H.F. Wehrl, J. Schwab, K. Hasenbach, G. Reischl, G. Tabatabai, L. Quintanilla-Martinez, F. Jiru, K. Chughtai, A. Kiss, F. Cay, D. Bukala, R.M. Heeren, B.J. Pichler, A.W. Sauter, Multimodal elucidation of choline metabolism in a murine glioma model using magnetic resonance spectroscopy and 11C-choline positron emission tomography, Cancer Res. 73 (5) (Mar 1 2013) 1470–1480.

[41] B.L. Miller, L. Chang, R. Booth, et al., In vivo 1H MRS choline: correlation with in vitro chemistry/histology, Life Sci. 58 (1996) 1929–1935.

[42] L. Chang, D. McBride, B.L. Miller, et al., Localized in vivo 1H magnetic resonance spectroscopy and in vitro analyses of heterogeneous brain tumors, J. Neuroimaging 5 (1995) 157–163.

[43] F. Imani, F.E. Boada, F.S. Lieberman, D.K. Davis, E.L. Deeb, J.M. Mountz, Comparison of proton magnetic resonance spectroscopy with fluorine- 18 2-fluoro-deoxyglucose positron emission tomography for assessment of brain tumor progression, J. Neuroimaging 22 (2012) 184–190.

[44] S. Saraswathy, F.W. Crawford, K.R. Lamborn, A. Pirzkall, S. Chang, S. Cha, et al., Evaluation of MR markers that predict survival in patients with newly diagnosed GBM prior to adjuvant therapy, J. Neuro-Oncol. 91 (2009) 69–81.

[45] A. Frati, A. Pichierri, S. Bastianello, A. Raco, A. Santoro, V. Esposito, et al., Frameless stereotactic cerebral biopsy: our experience in 296 cases, Stereotact. Funct. Neurosurg. 89 (2011) 234–245.

[46] S. Doblas, T. He, D. Saunders, J. Hoyle, N. Smith, Q. Pye, et al., In vivo characterization of several rodent glioma models by (1) H MRS, NMR Biomed. 25 (2012) 685–694.

[47] R.A. de Graaf, In Vivo Nmr Spectroscopy: Principles and Techniques, Wiley, 2007.

[48] M.A. Yorek, A.A. Spector, Taurine transport and metabolism in human retinoblastoma cells, Prog. Clin. Biol. Res. 179 (1985) 361–370.

[49] M.S. Starr, Uptake of taurine by retina in different species, Brain Res. 151 (1978) 604–608.

[50] L.I.A. Metwally, S.E. El-din, O. Abdelaziz, I.M. Hamdy, A.K. Elsamman, A.M. Abdelalim, Predicting grade of cerebral gliomas using Myo-inositol/Creatine ratio, Egypt. J. Radiol. Nucl. Med. 45 (1) (2014) 211–217.

[51] M.D. Krieger, A. Panigrahy, J.G. McComb, et al., Differentiation of choroid plexus tumors by advanced magnetic resonance spectroscopy, Neurosurg. Focus. 18 (6 A) (Jun 15 2005), E4.

[52] I.B. Yeh, M. Xu, W.H. Ng, et al., Central neurocytoma: typical magnetic resonance spectroscopy findings and atypical ventricular dissemination, Magn. Reson. Imaging 26 (1) (2008) 59–64.

[53] R.L. Kohl, J.R. Perez–Polo, W.B. Quay, Effect of methionine, glycine and serine on serine hydroxymethyl transferase activity in rat glioma and human neuroblastoma cells, J. Neurosci. Res. 5 (1980) 271–280.

[54] K. Sato, S. Yoshida, K. Fujiwara, K. Tada, M. Tohyama, Glycine cleavage system in astrocytes, Brain Res. 567 (1991) 64–70.

[55] S.D. Skaper, J.E. Seegmiller, Elevated intracellular glycine associated with hypoxanthine–guanine phosphoribosyltransferase deficiency in glioma cells, J. Neurochem. 29 (1977) 83–86.

[56] H. Bruhn, T. Michaelis, K.D. Merboldt, W. Hanicke, M.L. Gyngell, J. Frahm, 1991, monitoring cerebral glucose in diabetics by proton MRS, Lancet 337 (8743) (Mar 23 1991) 745–746.

[57] G.K. Radda, R.M. Dixon, C.A. Wood, NMR studies of phospholipid metabolism and cell proliferation, Biochem. Soc. Trans. 19 (1991) 995–996.

[58] A. Server, R. Josefsen, et al., Proton magnetic resonance spectroscopy in the distinction of high-grade cerebral gliomas from single metastatic brain tumors, Acta Radiol. 51 (3) (2010) 316–325.

[59] M.F. Chernov, Y. Ono, et al., Comparison of (1)H-MRS-detected metabolic characteristics in single metastatic brain tumors of different origin, Brain Tumor Pathol. 23 (1) (2006) 35–40.

[60] F.A. Howe, S.J. Barton, et al., Metabolic profiles of human brain tumors using quantitative in vivo 1H magnetic resonance spectroscopy, Magn. Reson. Med. 49 (2) (2003) 223–232.

[61] L. Porto, M. Kieslich, et al., MR spectroscopy differentiation between high and low grade astrocytomas: a comparison between paediatric and adult tumours, Eur. J. Paediatr. Neurol. 15 (3) (2011) 214–221.

[62] M. Law, S. Yang, et al., Glioma grading: sensitivity, specificity, and predictive values of perfusion MR imaging and proton MR spectroscopic imaging compared with conventional MR imaging, AJNR Am. J. Neuroradiol. 24 (10) (2003) 1989–1998.

[63] c. Majos, M. Julia-Sape, C. Arus, Usefulness of Proton Magnetic Resonance Spectroscopy in the Clinical Management of Brain Tumours, in: C.S.D. Rothman (Ed.), Magnetic Resonance Spectroscopy, Academic Press, San Diego 2014, pp. 141–161.

[64] W. Moller-Hartmann, S. Herminghaus, et al., Clinical application of proton magnetic resonance spectroscopy in the diagnosis of intracranial mass lesions, Neuroradiology 44 (5) (2002) 371–381.

[65] J.M. Roda, J.M. Pascual, F. Carceller, F. González-Llanos, A. Pérez-Higueras, J. Solivera, L. Barrios, S. Cerdán, Nonhistological diagnosis of human cerebral tumors by 1H magnetic resonance spectroscopy and amino acid analysis, Clin. Cancer Res. 6 (10) (Oct 2000) 3983–3993.

[66] A.P. Candiota, C. Majós, M. Julià-Sapé, M. Cabañas, J.J. Acebes, et al., Non-invasive grading of astrocytic tumours from the relative contents of myo-inositol and glycine measured by in vivo MRS, JBR-BTR 94 (6) (Nov-Dec 2011) 319–329.

[67] P. Weybright, P. Maly, D. Gomez-Hassan, C. Blaesing, P.C. Sundgren, MR spectroscopy in the evaluation of recurrent contrast-enhancing lesions in the posterior fossa after tumor treatment, Neuroradiology 46 (7) (Jul 2004) 541–549.

[68] Q.S. Zeng, C.F. Li, K. Zhang, H. Liu, X.S. Kang, J.H. Zhen, Multivoxel 3D proton MR spectroscopy in the distinction of recurrent glioma from radiation injury, J. Neuro-Oncol. 84 (1) (Aug 2007) 63–69.

[69] S. Chawla, Y. Zhang, et al., Proton magnetic resonance spectroscopy in differentiating glioblastomas from primary cerebral lymphomas and brain metastases, J. Comput. Assist. Tomogr. 34 (6) (2010) 836–841.

[70] W.G. Negendank, S.K. Padavic, C.W. Li, B.J. Murphy, R. Stoyanova, R.L. Krigel, R.J. Schilder, M.R. Smith, T.R. Brown, Metabolic characterization of human non-Hodgkin's lymphomas in vivo with the use of proton–decoupled phosphorus magnetic resonance spectroscopy, Cancer Res. 55 (1995) 3286–3294.

[71] M.K. Demir, A.C. Iplikcioglu, A. Dincer, M. Arslan, A. Sav, Single voxel proton MR spectroscopy findings of typical and atypical intracranial meningiomas, Eur. J. Radiol. 60 (1) (Oct 2006) 48–55.

[72] V. Tugnoli, L. Schenetti, A. Mucci, et al., Ex vivo HR-MAS MRS of human meningiomas: a comparison with in vivo 1H MR spectra, Int. J. Mol. Med. 18 (5) (2006) 859–869.

[73] A.R. Tate, J. Underwood, D.M. Acosta, et al., Development of a decision support system for diagnosis and grading of brain tumours using in vivo magnetic resonance single voxel spectra, NMR Biomed. 19 (4) (Jun 2006) 411–434.

[74] J.M. García-Gómez, J. Luts, M. Julià-Sapé, et al., Multiproject–multicenter evaluation of automatic brain tumor classification by magnetic resonance spectroscopy, MAGMA 22 (1) (Feb 2009) 5–18.

[75] A. Vellido, E. Romero, et al., Outlier exploration and diagnostic classification of a multi-centre 1H-MRS brain tumour database, Neurocomputing 72 (13–15) (2009) 3085–3097.

[76] F.G. Lehnhardt, G. Rohn, R.I. Ernestus, M. Grune, M. Hoehn, 1H- and (31)P-MR spectroscopy of primary and recurrent human brain tumors in vitro: malignancy-characteristic profiles of water soluble and lipophilic spectral components, NMR Biomed. 14 (2001) 307–317.

[77] B. Hubesch, D. Sappey-Marinier, K. Roth, et al., P-31 MR spectroscopy of normal human brain and brain tumors, Radiology 174 (1990) 401–409.

[78] J.W. Hugg, G.B. Matson, D.B. Twieg, et al., Phosphorus-31 MR spectroscopic imaging (MRSI) of normal and pathological human brains, Magn. Reson. Imaging 10 (1992) 227–243.

[79] D.L. Arnold, J.F. Emrich, E.A. Shoubridge, J.G. Villemure, W. Feindel, Characterization of astrocytomas, meningiomas and pituitary adenomas by phosphorus magnetic resonance spectroscopy, J. Neurosurg. 74 (1991) 447–453.

[80] R.D. Oberhaensli, D. Hilton-Jones, P.J. Bore, et al., Biochemical investigation of human tumors in vivo with phosphorus-31 magnetic resonance spectroscopy, Lancet 2 (8497) (1986) 8–11.

[81] C.M. Segebarth, D.F. Baleriaux, R. de Beer, et al., 1H image-guided localized 31P MR spectroscopy of human brain: quantitative analysis of 31P MR spectra measured on volunteers and on intracranial tumor patients, Magn. Reson. Med. 11 (1989) 349–366.

[82] T. Kaibara, R.L. Tyson, G.R. Sutherland, Human cerebral neoplasms studied using MR spectroscopy: a review, Biochem. Cell Biol. 76 (1998) 477–486.

[83] J.R. Griffiths, et al., Metabolic changes detected by in vivo magnetic resonance studies of HEPA-1 wild-type tumor deficient in hypoxia-inducible factor-1β (HIF-1β): evidence of an anabolic role for the HIF-1 pathway, Cancer Res. 62 (2002) 688–695.

[84] I. Tkáč;, G. Öz, G. Adriany, K. Uğ urbil, R. Gruetter, In vivo 1H NMR spectroscopy of the human brain at high magnetic fields: metabolite quantification at 4 T vs. 7 T, Magn. Reson. Med. 62 (4) (2009) 868–879.

[85] V.O. Boer, D.W. Klomp, C. Juchem, P.R. Luijten, R.A. de Graaf, Multislice (1) H MRSI of the human brain at 7 T using dynamic B(0) and B(1) shimming, Magn. Reson. Med. 68 (2012) 662–670.

[86] S. Bisdas, G.L. Chadzynski, C. Braun, J. Schittenhelm, M. Skardelly, G.E. Hagberg, T. Ethofer, R. Pohmann, G. Shajan, J. Engelmann, G. Tabatabai, U. Ziemann, U. Ernemann, K. Scheffler, MR spectroscopy for in vivo assessment of the oncometabolite 2-hydroxyglutarate and its effects on cellular metabolism in human brain gliomas at 9.4 T, J. Magn. Reson. Imaging (2016), http://dx.doi.org/10.1002/jmri.25221 ([Epub ahead of print] PubMed PMID: 26970248).

[87] T.L. Richards, S.R. Dager, H.S. Panagiotides, et al., Functional MR spectroscopy during language activation: a preliminary study using proton echo-planar spectroscopic imaging (PEPSI), Int. J. Neuroradiol. 3 (1997) 490.